

Cloning of an apparent splice variant of the rat *N*-methyl-D-aspartate receptor NMDAR1 with altered sensitivity to polyamines and activators of protein kinase C

(excitatory amino acid receptors/glutamate receptors/*Xenopus* oocyte expression/phorbol esters)

GUYLAINE M. DURAND*, PAUL GREGOR†, XIN ZHENG*, MICHAEL V. L. BENNETT*, GEORGE R. UHL†‡§, AND R. SUZANNE ZUKIN*

*Department of Neuroscience, Albert Einstein College of Medicine, 1300 Morris Park Avenue, Bronx, New York 10461; †Laboratory of Molecular Neurobiology, Addiction Research Center, National Institute on Drug Abuse, Baltimore, MD 21224; and ‡Departments of Neurology and Neuroscience, Johns Hopkins University School of Medicine, Baltimore, MD 21205

Contributed by Michael V. L. Bennett, July 6, 1992

ABSTRACT Molecular cloning identified complementary DNA species, from a rat ventral midbrain library, encoding apparent splice variants of the *N*-methyl-D-aspartate (NMDA) receptor NMDAR1 (which we now term NR1a). Sequencing revealed that one variant, NR1b, differs from NR1a by the presence of a 21-amino acid insert near the amino end of the N-terminal domain and by an alternate C-terminal domain in which the last 75 amino acids are replaced by an unrelated sequence of 22 amino acids. NR1b is virtually identical to NR1a in the remainder of the N- and C-terminal domains, at the 5' and 3' noncoding ends, and within the predicted transmembrane domains and extracellular and cytoplasmic loops. These findings suggest that the two forms of the receptor arise by differential splicing of a transcript from the same gene. Sequencing of other clones indicates the existence of a third variant, NR1c, identical to NR1b in its C terminus but lacking the N-terminal insert. NR1b RNA injected into *Xenopus* oocytes generated functional homomeric NMDA channels with electrophysiological properties distinct from those of NR1a homomeric channels. NR1b channels exhibited a lower apparent affinity for NMDA and for glutamate. NR1b channels exhibited a lower affinity for D-2-amino-5-phosphonovaleric acid and a higher affinity for Zn²⁺. The two receptor variants showed nearly identical affinities for glycine, Mg²⁺, and phenylcyclidine. Spermine potentiation of NMDA responses, prominent in oocytes injected with rat forebrain message, was also prominent for NR1a receptors, but was greatly reduced or absent for NR1b receptors. Treatment with the protein kinase C activator phorbol 12-myristate 13-acetate potentiated NMDA responses in NR1b-injected oocytes by about 20-fold; potentiation of NMDA responses in NR1a-injected oocytes was much less, about 4-fold. These findings support a role for alternate splicing in generating NMDA channels with different functional properties.

Glutamate is the primary excitatory neurotransmitter in the central nervous system. Channel-forming glutamate receptors in rat are encoded by about 20 identified genes in at least four gene subfamilies, GluR1 to GluR4 [encoding kainate/ α -amino-3-hydroxy-5-methyl-4-isoxazole-4-propionic acid receptors (1–4)], GluR5, GluR6, and KA [kainate receptors (5–7)], and NMDAR [*N*-methyl-D-aspartate (NMDA) receptors (8, 9)]. In recent years the NMDA receptor has attracted considerable interest due to its proposed roles in long-term potentiation (e.g., ref. 10), synaptogenesis, and developmental structuring (11). Moreover, NMDA receptor-mediated toxicity is thought to represent a final common pathway for

the neurodegeneration associated with a wide range of neurological insults including trauma, hypoglycemia, ischemia, and epilepsy, as well as Alzheimer disease and Huntington disease (12).

The recently cloned NMDA receptors from rat, NMDAR1 (8) and NMDAR2A-C (9), belong to the large superfamily of ligand-gated ion channels. Analyses of the predicted protein sequences reveal characteristic structural motifs including a large extracellular N-terminal domain, a small extracellular C-terminal domain, four transmembrane domains (the second of which is flanked by negatively charged residues and is thought to line the ion channel), and possible phosphorylation sites within the second cytoplasmic loop. The NMDAR1 receptor exhibits significant amino acid homology with other glutamate receptors, particularly evident in the hydrophobic membrane-spanning regions, and is more distantly related to other members of the ligand-gated superfamily. The diversity of functions associated with NMDA receptor activation could reflect the existence of multiple NMDA receptor subtypes or splice variants.

Here we report the identification and cloning of cDNAs[¶] encoding apparent splice variants of the rat NMDAR1 receptor, which we now term NR1a. One receptor variant, NR1b, differs from NR1a by the insertion of 21-amino acid residues near the amino end of the N-terminal domain and the presence of an alternate C-terminal domain. The C-terminal replacement arises from a nucleotide deletion that includes the stop codon of NR1a and leads to formation of a new open reading frame. These structural differences impart to NR1b receptors a severalfold lower affinity for agonists, reduced potentiation by the polyamine, spermine, and increased potentiation by activators of protein kinase C (PKC). Another variant, NR1c, has the C-terminal modification but lacks the N-terminal insertion.

MATERIALS AND METHODS

cDNA Cloning. To isolate cDNAs encoding NMDA receptor subtypes, we used a size-selected (>2.5-kilobase insert size) ventral midbrain cDNA library constructed in the λ ZAP vector (13). The library was screened with a 441-base fragment of the rat NR1a receptor cDNA (8), obtained by PCR. Two degenerate oligonucleotide primers constructed according to amino acid sequences 495–502 (KKEWNGMM in the

Abbreviations: APV, D-2-amino-5-phosphonovaleric acid; NMDA, *N*-methyl-D-aspartate; PKC, protein kinase C; PMA, phorbol 12-myristate 13-acetate.

§To whom reprint requests should be sent at: P.O. Box 5180, Baltimore, MD 21224.

¶The sequence reported in this paper has been deposited in the GenBank data base (accession no. L01632).

The publication costs of this article were defrayed in part by page charge payment. This article must therefore be hereby marked "advertisement" in accordance with 18 U.S.C. §1734 solely to indicate this fact.

N-terminal region just preceding the transmembrane domain) and 634–641 (MVWAGFAM in the third transmembrane domain) of NR1a were used to PCR amplify homologous sequences from rat midbrain cDNA (see Fig. 1A). The amplified DNA, apparently a single species corresponding to amino acids 495–641 of NR1a, was excised from the gel, subcloned, radiolabeled by random priming, and used to screen the rat ventral midbrain cDNA library. Hybridization was performed in 3× standard saline citrate buffer containing 29% formamide (18 h at 37°C). Plasmids were rescued from λZAP clones by autoexcision as described (13). Nucleotide sequence analysis was performed on denatured double-stranded templates by manual and automated sequencing (13).

Oocyte Methods. Oocytes were removed from the ovarian lobes of anesthetized *Xenopus laevis*, defolliculated, injected with NR1a or NR1b RNA (50 ng per cell), and maintained at 18°C (14, 15). The NR1a clone was obtained from Shigetada Nakanishi (Kyoto, Japan). After 4 or 5 days, oocytes were placed in a recording chamber and perfused with Mg²⁺-free ND-96 solution (116 mM NaCl/2.0 mM KCl/0.5 mM CaCl₂/10 mM Hepes, pH 7.2). Drugs were applied by bath perfusion during recording under two-electrode voltage clamp (14, 15).

RESULTS

Isolation and Characterization of NR1b and Identification of NR1c. A cDNA library of rat ventral tegmentum and mid-brain was screened using the 441-base fragment of NR1a obtained by PCR, as described in *Materials and Methods*. Twenty clones hybridized to the NR1a fragment. Restriction analysis with *EcoRI* indicated that one clone differed from NR1a. This clone, NR1b, was found by an initial nucleotide sequence analysis to be identical to NR1a in the 5' untranslated region, which originates at nucleotide -19 of NR1a, and in the distal 3' untranslated region, which extends to nucleotide 3946 of NR1a (8).

Further sequence analysis demonstrated that NR1b differs from NR1a at two principal locations (Fig. 1A). As discussed further below, these differences are likely to result from alternate splicing. NR1b contains an additional 63-base sequence encoding a 21-amino acid insert within the predicted N-terminal domain (Fig. 1A). NR1b also lacks 467 bases in the region corresponding to the end of the predicted C-terminal domain and extending beyond the stop codon of NR1a. This deletion removes the last 75 codons and more than 240 bases of the 3' noncoding region and yields a different open reading frame that encodes an additional 22 amino acids before a stop codon is reached at a position corresponding to nucleotide 3123 of NR1a (Fig. 1C).

The insert within the predicted N-terminal domain of NR1b is enriched in basic amino acid residues. The C terminal of NR1b contains a consensus sequence for asparagine-linked glycosylation not present in NR1a (asterisk in Fig. 1A). NR1b has an additional minor variation with respect to NR1a, a silent mutation of guanine to adenine at base 1584 of NR1a, which creates an *EcoRI* site at codon 549 of NR1b (arrowhead in Fig. 1A). The presence of several additional silent mutations was suggested by single-strand sequencing but was not confirmed.

NR1b and NR1a are virtually identical in their common 3' and 5' noncoding regions and in the regions encoding the predicted transmembrane domains, the extracellular and cytoplasmic loops, and the N- and C-terminal domains except for the differences noted above. Thus, they most likely arise as a result of alternate splicing of the primary transcripts of a single gene. However, the silent mutation at nucleotide 1584 of NR1a and probably several others may represent alleles of the rat NMDAR1 gene.

A

```

1  MSTMHLLTFA LLESCSEARA ACDPKVINIG AVLSTRKHEQ MFREAVNQAN
51  KRHGSWKIQL NATSVTHKPN AIQMALSVCE DLISSQVYAI LVSHPPPTFD
101 HFTPTFVSYT AGFYRIPVLG LTRMSIYSD KSIHLSFLRT VPPYSHQSSV
151 WFEMRVYNW NHIIILLVSD HEGRAAQKRL ETLLERESK SEKKNYKELD
201 QLSYDNKNGP KAEKVLQDFP GKNVTALML EARELEARVI ILSASEDDAA
251 TVYRAAAMLN MTGSGYVWLW GERETISGNL RYAPDGIIGL QLINGKNESA
301 HISDAVGVA QAVHELLEKE NITDPPRGCV GNTNIWKTGP LFKRVLMSK
351 YADGVTGRVE FNEDGDRKFA NYSIMNLQNR KLVQVGIYNG THVIPNDRKI
401 IMPGGETEKP RGYQMSTRLK IVTIHQEPFV YVKPTMSDGT CKEEPTVNGD
451 PVKVICITGF NDTSPGSPRH TVPQCCYGF IDLLIKLART MNFTYEVHLV
501 ADGKFGTQER VNNSNKKEMW GMMGELLSSG ADMIVAPLTI NNERAQYIEF
551 SKPFYQGLT ILVKEIPRS TLDSEMPQFF STLWLVGLHS VVAVMLYL
601 LDRFSPFGRF KVNSEEEED ALTLSSAMFE SMGVLLNSGI GEGAPRFSFA
651 RILGMVWAGE AMLIIVASYTA NLAAPLVLDR PEERTGTIND PRLRNPDKF
701 IYATVKQSSV DIYFRQVEL NTYRHEKHX NYESAAEAIQ AVRDNKLDHF
751 IWDSAVLEFE ASQKCDLVTT GELFFRSRGF IGMKRDSPWK QNVSLSLKLS
801 HENGFMEDLD KTWVRYQECD SRSNAPATLT FENMAGVFMV VAGGIVAGIE
851 LIEIEIAYKR HKDARRKQMQ LAFAAVNVWR KNIQQYKPTD ITGFLILSDP
901 SVSTVV

```

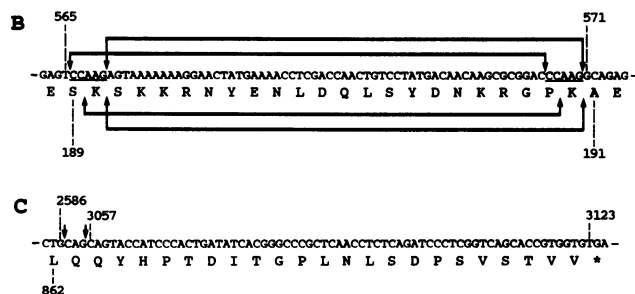


FIG. 1. Predicted amino acid sequence of NR1b and summary of differences in nucleotide sequences between NR1b and NR1a. (A) The predicted amino acid sequence. The 22-amino acid insert into NR1b at residue 190 (or 189) is indicated in boldface letters; because of repetition of the lysine residue it has two equivalent sequences indicated by connected arrows. The alternate C terminus is indicated in boldface letters. The added asparagine-linked glycosylation site is indicated by an asterisk. Also indicated by underlining are the putative signal peptide (SP) and the four membrane-spanning regions (TM1–TM4). The site of the PCR-generated probe is indicated by bent arrows. The *EcoRI* restriction site in the cDNA is at the codon for the amino acid indicated by an arrowhead. (B) The site of the insert showing both the coding and amino acid sequences (numbered according to NR1a; ref. 8). Because the coding sequence in the insert region starts and ends with the underlined sequence, **CCAAG**, the exact site at which a single exon inclusion could occur cannot be determined from the nucleotide sequence. There are six possible splice sites between bases 566 and 572 of NR1a. For each site the presumptive exon differs at its 5' and 3' ends, so as to give the same final sequence. The connected arrows over the nucleotide sequence indicate the extreme 5' and 3' possible sites of the insertion and the corresponding exon sequences. The connected pairs of arrows under the amino acid sequence indicate the two possible sequences of the resulting amino acid insert. (C) The alternate C-terminal coding and amino acid sequences (numbered according to NR1a). Because the four bases in NR1a after base 2585 are the same as those before base 3057, there are five possible sites (two of which are indicated by arrows) at which a presumptive single exon could be omitted and five corresponding starts of the following sequences.

Five additional cDNAs, likely to be independent clones on the basis of differing sizes, were found by partial nucleotide sequence analysis to have the same C-terminal deletion as NR1b (data not shown) but not the N-terminal addition. Thus, there must be at least one other variant, which we provisionally term NR1c.

NR1b Directs the Translation of Functional NMDA Receptors. The functional properties of NR1b and NR1a homo-

meric channels were compared by voltage-clamp analysis following expression of the corresponding RNAs in *Xenopus* oocytes. NR1b responses to NMDA (300 μ M with 10 μ M glycine) and to glutamate (100 μ M with 10 μ M glycine) were characterized by an initial peak inward current that decayed to a steady-state level, similar to NR1a responses (Fig. 2A; ref. 8). Concentration-response relations were determined for the activation of NR1b and NR1a receptors (Fig. 3). The apparent affinity of NR1b for NMDA was about 5-fold lower than that of NR1a (Table 1). The calculated Hill coefficients did not differ significantly (1.15 ± 0.04 for NR1b, 1.03 ± 0.03 for NR1a). The apparent affinity of NR1b for glutamate was also lower than that of NR1a (Table 1). These data demonstrate that the subunits form functional homomeric channels with different affinities for NMDA and L-glutamate. We saw no evidence of formation of heteromeric channels in oocytes coinjected with NR1a (25 ng) and NR1b (25 ng).

The sensitivity of the channels encoded by NR1b to other glutamate receptor agonists and antagonists was also investigated. Oocytes injected with NR1b RNA showed no response to kainate (100 μ M) or to quisqualate (100 μ M; data not shown). NR1b responses to NMDA were blocked by APV (Fig. 2B). The IC_{50} for APV at NR1b receptors was about 1.6 times that at NR1a receptors (Table 1). The two variants showed the same apparent affinities for glycine.

NMDA responses in oocytes expressing NR1b receptors were blocked by Mg^{2+} (100 μ M) in a voltage-dependent manner (data not shown). The reversal potential (-20 mV) was the same with and without Mg^{2+} (Table 1). The IC_{50} for

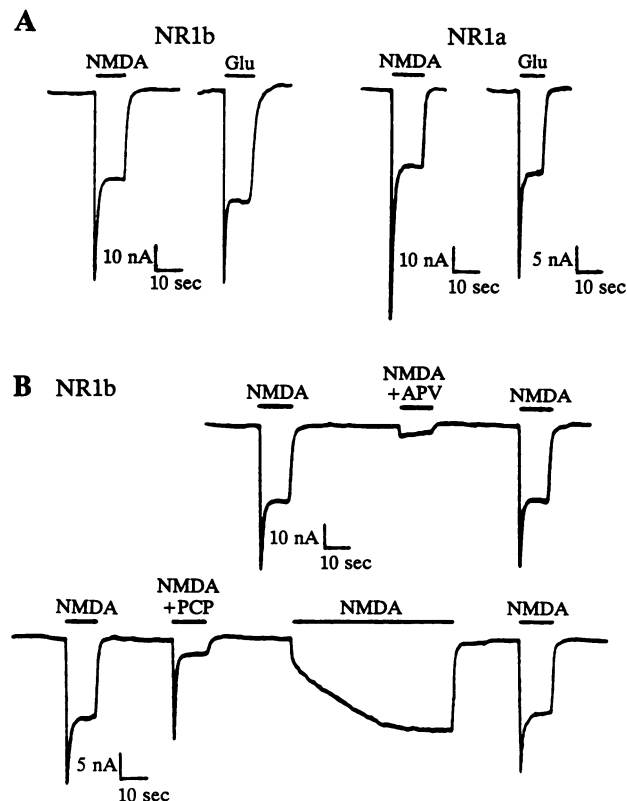


FIG. 2. NR1a and NR1b each directs the synthesis of functional NMDA receptors in *Xenopus* oocytes. (A) Inward current responses to application of NMDA (300 μ M with 10 μ M glycine) and L-glutamate (Glu; 100 μ M with 10 μ M glycine) are shown. Membrane potential was held at -100 mV. Each record is from a different oocyte. (B) Responses of NR1b receptors to NMDA (300 μ M with 10 μ M glycine) were blocked by the competitive antagonist D-2-amino-5-phosphonovaleric acid (APV; 100 μ M) and showed typical use-dependent block and recovery upon application of the channel blocker phencyclidine (PCP; 100 nM).

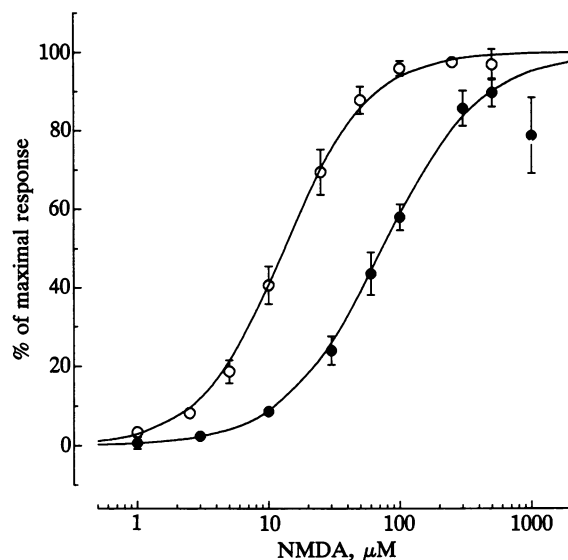


FIG. 3. Concentration-response relations for NMDA of NR1b (\bullet) and NR1a (\circ) receptors. Responses were normalized to the maximal current calculated by fit by nonlinear regression to the Hill equation, excluding the point at the highest concentration for each clone at which desensitization may have been occurring. Each point represents the mean (\pm SD) of agonist-evoked currents measured in triplicate in eight different oocytes, voltage clamped at -100 mV.

Mg^{2+} at a holding potential of -60 mV was the same at NR1b and NR1a receptors. The IC_{50} for Zn^{2+} was about 2-fold lower for NR1b than for NR1a. The IC_{50} for phencyclidine was the same for the two receptor variants. All these properties of homomeric NMDA channels are very similar to those of NMDA channels expressed in oocytes injected with rat brain mRNA (14) or to those of neuronal NMDA channels (17, 18).

Potentiation by the Polyamine, Spermine. Spermine differentially affected NR1a and NR1b responses. At -60 mV and saturating glycine (10 μ M), spermine (250 μ M) reversibly potentiated NR1a responses (Fig. 4B), as was observed in oocytes expressing rat forebrain mRNA (19) and cortical neurons (20). However, under these conditions, spermine produced at most a small inhibition of NR1b responses (Fig. 4A). At a more hyperpolarized potential (-100 mV), spermine produced a modest inhibition of NR1a responses (plateau phase) and a more pronounced inhibition of NR1b

Table 1. Functional properties of NR1a and NR1b homomeric channels expressed in *Xenopus* oocytes

Ligand	NR1b		NR1a	
	EC_{50} or IC_{50}^{\dagger}	<i>n</i>	EC_{50} or IC_{50}^{\dagger}	<i>n</i>
NMDA	67 ± 1.5	8	13.2 ± 0.9	6***
Glutamate	5.6 ± 1.2	3	1.7 ± 0.2	3*
APV	2.5 ± 0.3	5	1.6 ± 0.1	6*
Glycine	0.90 ± 0.12	8	1.0 ± 0.10	5
Mg^{2+}	28 ± 7	4	27 ± 6	4
Zn^{2+}	34 ± 4.3	4	56 ± 3	3**
Phencyclidine	22 ± 3.4	4	17 ± 2.4	2

Values are means \pm SEM of mean responses for single oocytes. *n*, Number of oocytes. NMDA and glutamate were applied with 10 μ M glycine. Antagonists were applied with NMDA (300 μ M) and glycine (10 μ M). For APV the measured value, IC_{50}^{\dagger} , was corrected for NMDA concentration, [NMDA], and apparent affinity, $EC_{50,NMDA}$, according to the equation $IC_{50} = IC_{50}^{\dagger} / (1 + [NMDA] / EC_{50,NMDA})$. Significance was determined by Student's *t* test. *, $P < 0.05$; **, $P < 0.01$; ***, $P < 0.0001$.

\dagger Values are micromolar except for phencyclidine, which is nanomolar.

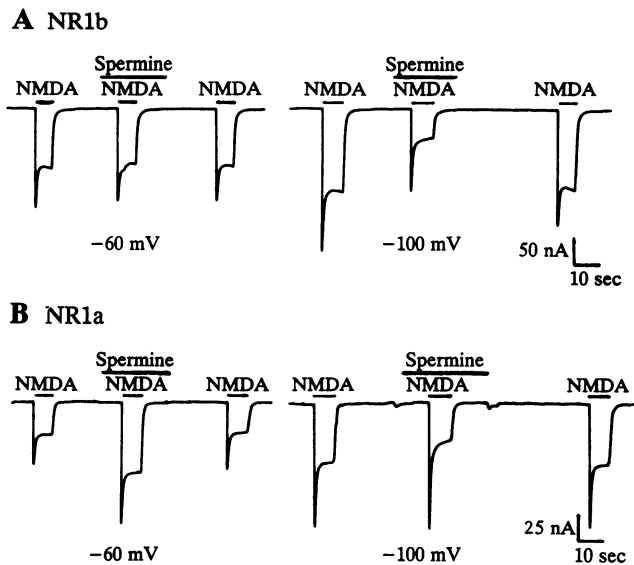


FIG. 4. Spermine differentially modulates NR1b and NR1a receptors. (A) At -60 mV, spermine ($250 \mu\text{M}$) slightly reduced the NR1b response to NMDA ($300 \mu\text{M}$ with $10 \mu\text{M}$ glycine). At -100 mV, spermine markedly reduced the response. (B) At -60 mV, spermine ($250 \mu\text{M}$) potentiated the NR1a response to NMDA. At -100 mV, spermine reduced the plateau phase of the response.

responses. At low glycine ($0.1 \mu\text{M}$; cf. ref. 19) and at -70 mV or more positive potentials, spermine produced increased potentiation of NR1a responses and a modest potentiation of NR1b responses (data not shown).

Modulation of Channel Activity by PKC Activators. The PKC activator phorbol 12-myristate 13-acetate (PMA; 10 nm or $1 \mu\text{M}$) potentiated NR1b responses to NMDA ($300 \mu\text{M}$) by about 15- to 20-fold (Fig. 5A and Table 2). The effect required minutes to develop. Potentiation by PMA ($1 \mu\text{M}$) of NR1a responses or of responses of receptors expressed from rat

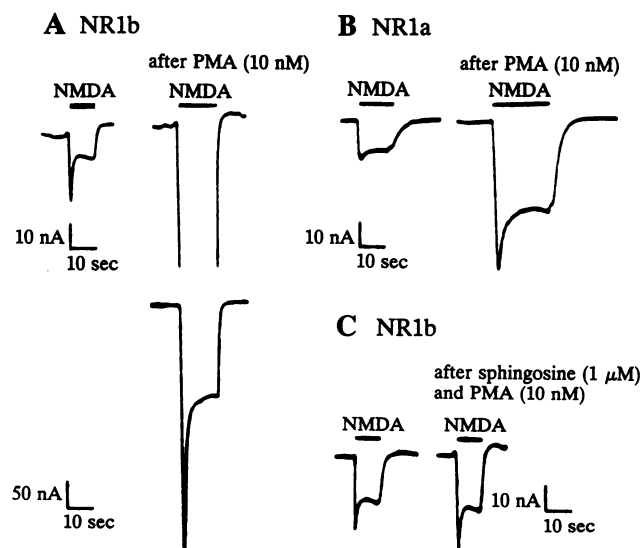


FIG. 5. PMA potentiates responses of NR1b and NR1a receptors differentially. (A) PMA potentiated NR1b responses to NMDA ($300 \mu\text{M}$ with $10 \mu\text{M}$ glycine) in *Xenopus* oocytes by about 20-fold. Responses to NMDA ($300 \mu\text{M}$) before (Left) and after (Right) a 10-min treatment with 10 nM PMA; high and low gains are shown in upper and lower traces, respectively. (B) PMA potentiated this NR1a response to NMDA much less, about 3-fold. (C) Potentiation of NR1b responses by 10 nM PMA was almost completely blocked by a 15-min pretreatment with sphingosine ($1 \mu\text{M}$) followed by coapplication of sphingosine and PMA for 10 min.

Table 2. Effect of kinase modulators on responses of NR1b receptors

Compound	Action	Treated/control, mean \pm SEM	n
PMA ($1 \mu\text{M}$)	PKC activator (phorbol ester)	19 ± 4.6	6
PMA (10 nM)		15 ± 2.9	3
Mezerein ($1 \mu\text{M}$)	PKC activator (diterpene)	16 ± 1	2
Mezerein (100 nM)		8 ± 0	2
4α -Phorbol ($1 \mu\text{M}$)	Inactive form of PMA	1	4
8-Br-cAMP (1 or 3 mM)	PKA activator	1	2
Forskolin (5 or $10 \mu\text{M}$)	PKA activator	1	3
PMA (10 nM) + staurosporine ($1 \mu\text{M}$)	PKC inhibitor	2 ± 0.3	2
PMA (10 nM) + sphingosine ($1 \mu\text{M}$)	PKC inhibitor	1 ± 0.2	2

Steady-state currents elicited by application of NMDA ($300 \mu\text{M}$) with glycine ($10 \mu\text{M}$) were recorded from oocytes injected with NR1b RNA, after a 10-min treatment with compounds as indicated. Potentiation is measured as the ratio of steady-state responses to NMDA after and before treatment with the compound(s) indicated.

brain mRNA was much less (4.5- and 4-fold, respectively, $P < 0.01$ vs. NR1b by *t* test; see also Fig. 5B). Application of mezerein, a nonphorbol PKC activator, also produced a marked potentiation of the NMDA response of NR1b receptors (Table 2). The effect of PMA was almost completely blocked by preapplication of the PKC inhibitors staurosporine ($1 \mu\text{M}$) and sphingosine ($1 \mu\text{M}$; Fig. 5C and Table 2). No effect was produced by an inactive phorbol ester 4α -phorbol ($1 \mu\text{M}$) or by the protein kinase A activators 8-Br-cAMP (3 mM) and forskolin ($10 \mu\text{M}$).

DISCUSSION

Our study demonstrates the presence of at least three apparent splice variants of the NMDAR1 receptor in rat brain. NR1b differs from NR1a by the presence of an additional 63 nucleotides in the N-terminal domain encoding 21 amino acids and the absence of 467 nucleotides in the distal end and downstream from the coding region of NR1a. This deletion results in replacement of the last 75 amino acids with an unrelated sequence of 22 amino acids, and part of the noncoding sequence of NR1a is converted into coding sequence in NR1b. That NR1b is virtually identical to NR1a in the coding and noncoding regions except for these differences indicates that the two forms of the receptor arise by differential splicing of a primary transcript of the same gene. NR1c has the deletion, but not the insert, which is a further indication of alternate splicing.

The functional differences between NR1b and NR1a are marked and include differences in agonist affinity and potentiation by spermine and PKC activators. A 100-amino acid segment within the predicted N-terminal domain of other glutamate receptor subtypes is implicated in agonist binding (4, 21). Although NR1b has reduced agonist affinity, its modifications relative to NR1a are not in this region and may affect the site through alterations in the secondary and tertiary structure of the protein. Synapses with homomeric NR1b receptors would exhibit reduced responses to glutamate and potentiation by spermine but enhanced potentiation by PKC.

Cell-specific alternate splicing may underlie the variation in polyamine action observed in three studies of different central nervous system regions (20, 22, 23). Two of these studies (20, 23) indicate a dual action for spermine. At

hyperpolarized potentials and relatively high concentrations, spermine reduces NMDA single-channel conductance by rapid channel block or charge screening; the reduction is negligible at -40 mV. Spermine also increases mean open time (20), accounting for the potentiation seen at less hyperpolarized potentials. Our finding that NR1b receptors exhibit much less spermine potentiation at high glycine compared to NR1a, but stronger inhibition at hyperpolarized potentials, provides further support for the existence of independent sites for potentiation and reduction in single-channel conductance.

Several findings indicate that PMA potentiates NR1b and NR1a responses by activation of PKC: (i) PMA and mezerein produce potentiation at nanomolar concentrations, (ii) the onset of activation by PMA is delayed, and (iii) PMA potentiation is greatly reduced by the PKC inhibitors staurosporine and sphingosine. Other studies have suggested that activation of PKC leads to potentiation of NMDA responses (16, 24, 25).

Alternate splicing in the region encoding the C terminus is found in other glutamate receptors. The mouse has two variants of NR1, $\zeta 1$, which is nearly identical to NR1a, and a shorter form, $\zeta 1-2$ (25). $\zeta 1-2$ exhibits a deletion in the predicted amino acid sequence that starts at the same residue as in NR1b, but extends only 37 amino acids, leaving the final 38 residues unchanged. $\zeta 1$ has two adjacent possible sites at which a single exon could be omitted, at bases corresponding to 3056 and 3057 of NR1a. The high degree of conservation between rat and mouse suggests that one of these bases is likely to be the splice site for rat as well. However, the nucleotide deletion in $\zeta 1-2$ is much shorter than the nucleotide deletion in NR1b. There may be an additional splice variant in rat corresponding to mouse $\zeta 1-2$. No functional differences, including in potentiation by spermine and PKC activators, were noted for the mouse ζ variants with respect to each other or to NR1a (25).

GluR4, which has "flip" and "flop" splice variants (26), also has a C-terminal variant, GluR4c, affecting the C terminal (27). Apparently, inclusion of an exon causes replacement of the terminal 54 amino acids of GluR4 by a shorter, unrelated sequence of 36 amino acids. Interestingly, the C-terminal region of GluR4c is highly similar to that of GluR2 and GluR3, but not of GluR4 or GluR1. Assays of function showed differences between flip and flop variants of GluR1 and GluR3 (26), but were not noted for GluR4c compared to GluR4 (27). It is of interest with respect to region-specific regulation of alternate splicing that none of the six basal midbrain cDNAs sequenced by us is identical to NR1a, which was cloned from a rat forebrain cDNA library (8).

Our study shows that NR1b and NR1a receptors differ in agonist and antagonist affinity and in potentiation by the polyamine, spermine, and activators of PKC. It remains to be determined which differences between NR1b and NR1a are functionally relevant. Where differences are not detected electrophysiologically, receptor variants may differ in other aspects such as assembly or localization on the cell surface. Clearly, the presence of different receptor splice variants is one factor that may contribute to differences in glutamatergic synaptic transmission.

Note Added in Proof. Two additional reports of apparent splice variants of NR1 have now appeared (28, 29) and are in agreement with (and complement) our sequence data. Together, their and our studies are consistent with the presence of three exons that can be independently spliced in, one encoding the N-terminal insert of NR1b and two that together comprise the deletion in NR1b and NR1c.

We thank Ms. Maria Rutto, Rosa Grieco, and Carol Sheeringer for secretarial help; Mr. Peter Yellin and Xiaodong Yang for technical assistance; and Roxanne Ingersoll for automated sequencing. We are grateful to Dr. Shigetada Nakanishi for supplying us with the NR1a clone. This work was supported in part by National Institutes of Health Grant NS 20752 to R.S.Z., Grants NS 07412 and HD 04248 to M.V.L.B., and by the intramural program of the National Institute on Drug Abuse. M.V.L.B. is the Sylvia and Robert S. Olnick Professor of Neuroscience.

- Hollman, M., O'Shea-Greenfield, A., Rogers, S. W. & Heinemann, S. (1989) *Nature (London)* **342**, 643-648.
- Boulter, J., Hollman, M., O'Shea-Greenfield, A., Hartley, M., Deneris, E., Maron, C. & Heinemann, S. (1990) *Science* **249**, 1033-1037.
- Keinanen, K., Wisden, W., Sommer, B., Werner, P., Herb, A., Verdoorn, T. A., Sakmann, B. & Seeburg, P. H. (1990) *Science* **249**, 556-560.
- Nakanishi, N., Schneider, N. A. & Axel, R. (1990) *Neuron* **5**, 569-581.
- Werner, P., Voight, M., Keinanen, K., Wisden, W. & Seeburg, P. H. (1991) *Nature (London)* **351**, 742-744.
- Bettler, B., Boulter, J., Hermans-Borgmeyer, I., O'Shea-Greenfield, A., Deneris, E., Moll, C., Borgmeyer, U., Hollman, M. & Heinemann, S. (1990) *Neuron* **5**, 583-595.
- Egebjerg, J., Bettler, B., Hermans-Borgmeyer, I. & Heinemann, S. (1991) *Nature (London)* **351**, 745-748.
- Moriyoshi, K., Masu, M., Ishii, T., Shigemoto, R., Mizuno, N. & Nakanishi, S. (1991) *Nature (London)* **354**, 31-37.
- Monyer, H., Sprengel, R., Schoepfer, R., Herb, A., Higuchi, M., Lomeli, H., Burnashev, N., Sakmann, B. & Seeburg, P. H. (1992) *Science* **256**, 1217-1221.
- Lynch, G. & Baudry, M. (1991) *Hippocampus* **1**, 9-14.
- Mattson, M. P., Dou, P. & Kater, S. B. (1988) *J. Neurosci.* **8**, 2087-2100.
- Choi, D. W., Koh, J. & Peters, S. (1988) *J. Neurosci.* **8**, 185-196.
- Shimada, S., Kitayama, S., Lin, C.-L., Patel, A., Nanthakumar, E., Gregor, P., Kuhar, M. & Uhl, G. (1991) *Science* **254**, 576-578.
- Kushner, L., Lerma, J., Zukin, R. S. & Bennett, M. V. L. (1988) *Proc. Natl. Acad. Sci. USA* **85**, 3250-3254.
- Kushner, L., Lerma, J., Bennett, M. V. L. & Zukin, R. S. (1989) in *Methods in Neuroscience*, ed. Conn, P. M. (Academic, Orlando), pp. 1-29.
- Kelso, S., Nelson, T. & Leonard, J. (1992) *J. Physiol. (London)* **449**, 705-718.
- Ascher, P. & Nowak, L. (1988) *J. Physiol. (London)* **399**, 247-266.
- Mayer, M. L. & Westbrook, G. L. (1987) *Prog. Neurobiol.* **28**, 197-270.
- McGurk, J., Bennett, M. V. L. & Zukin, R. S. (1990) *Proc. Natl. Acad. Sci. USA* **87**, 9971-9974.
- Rock, D. & Macdonald, R. (1992) *Mol. Pharmacol.* **41**, 83-88.
- Mishina, M., Sakimura, K., Mori, H., Kushiya, E., Harabayashi, M., Uchino, S. & Nagahari, K. (1991) *Biochem. Biophys. Res. Commun.* **180**, 813-821.
- Lerma, J. (1992) *Neuron* **8**, 343-352.
- Araneda, R., Zukin, R. & Bennett, M. V. L. (1991) *Soc. Neurosci. Abstr.* **17**, 1167.
- Chen, L. & Huang, L.-Y. M. (1992) *Nature (London)* **356**, 521-523.
- Yamazaki, M., Mori, H., Araki, K., Mori, K. & Mishina, M. (1992) *FEBS Lett.* **300**, 39-45.
- Sommer, B., Keinanen, K., Verdoorn, T. A., Wisden, W., Burnashev, N., Herb, A., Kohler, M., Takagi, T., Sakmann, B. & Seeburg, P. H. (1990) *Science* **249**, 1580-1585.
- Gallo, V., Upson, L. M., Hayes, W. P., Vyklicky, L., Jr., Winters, C. A. & Buonanno, A. J. (1992) *Neuroscience* **12**, 1010-1023.
- Anantharam, V., Panchal, R. G., Wilson, A., Kolchine, V. V., Triestman, S. N. & Bayley, H. (1992) *FEBS Lett.* **305**, 27-30.
- Sugihara, H., Moriyoshi, K., Ishii, T., Masu, M. & Nakanishi, S. (1992) *Biochem. Biophys. Res. Commun.* **185**, 826-832.